Collective topological dynamics in the Frenkel-Kontorova chains

Zhigang Zheng[1,2] and Bambi Hu[2,3]
[1]*Department of Physics, Beijing Normal University, Beijing 100875, China*
[2]*Department of Physics and Center for Nonlinear Studies, Hong Kong Baptist University, Hong Kong, China*
[3]*Department of Physics, University of Houston, Houston, Texas 77204*
(Received 28 July 1999; revised manuscript received 31 March 2000)

Topological dynamics of an array of harmonically coupled damped dc-driven nonlinear oscillators are studied by introducing a dynamical contraction factor and a deviation factor. Different dynamical transitions are identified, and topological changes for these transitions are studied. A bifurcation from the kink state to the kink-antikink-pair state is found, which relates the topological change to the spatiotemporal dynamics of the system. The presence of antikinks leads to the extension of the localized kink, and collisions of kinks and antikinks induce strong oscillations of the topology of the array.

PACS number(s): 45.05.+x, 05.45.−a, 74.40.+k, 74.50.+r

I. INTRODUCTION

There has been a great tide of interest in recent years in exploring collective behaviors of coupled nonlinear systems with spatiotemporally competing interactions [1,2] in relating to a number of practical problems in physics [3–5], biology [6], and chemistry [7]. The Frenkel-Kontorova (FK) model, which describes an array of N single pendula interacting with the harmonic nearest-neighboring coupling, may be one of the simplest capable of capturing the essential features of the competitive interactions [8]. In the damped case, when the array is driven by a constant external force, the equation of motion can be written as follows:

$$\ddot{\theta}_i+\gamma\dot{\theta}_i+\sin\theta_i=K(\theta_{i+1}-2\theta_i+\theta_{i-1})+I. \tag{1}$$

Here θ_i denotes the phase of the ith oscillator, and $\dot{\theta}_i$ its corresponding phase velocity. γ, K, and I are the friction coefficient, coupling strength, and constant driving force, respectively. The frustration, $\delta=\alpha/2\pi$, which relates to the spring constant α, does not appear in Eq. (1), but this parameter may play a significant role in the dynamics of system (1).

Despite its simplicity, the dynamical FK model has been fully investigated in relating to a number of problems, such as coupled pendula [9], charge-density waves [10], nanotribology and surface problems [11], the heat-conduction problem [12], synchronizations [13], coupled ratchets [14], and Josephson-junction arrays and ladders [15]. The ground state of the FK model has been exhaustively explored over the past few decades [16]. Dynamics of the FK model under various external influences such as dissipations, external dc and ac forces, and noises have been studied and abundant dynamical transitions and phase-locking behaviors were observed [5,17,18].

Under a constant drive I, the array may possess a nonzero value of the average velocity defined by

$$\Omega=\frac{1}{N}\sum_{j=1}^{N}\lim_{T\to\infty}\frac{1}{T}\int_0^T\dot{\theta}_j(t)dt. \tag{2}$$

It was shown that there is a gap between the low- and high-velocity regimes (LVR and HVR), where motions within these two regimes are distinguished by two types of wave propagations. In the LVR, the motion is dominated by the localized solitary wave (kinks). Due to the discreteness of the array, the velocity of the array may experience numerous resonant steps as one increases the external driving I [15,17]. In the HVR, the moving kink is strongly extended, where the whirling instability induces resonances in the HVR.

In spite of numerous studies in LVR and HVR, a quantitative description of the topology of the array is still lacking. Especially, it is an interesting issue about the configurational dynamics of the chain varying with external parameters and the manifestation of the topology during dynamical transitions [19]. The studies of these problems may shed light on collective behaviors of coupled systems with spatiotemporal competitions. The configurational behaviors of the spatially modulated systems such as the FK model have been fully studied in relating to the ground-state problem and the commensurate-incommensurate phase transitions. As for the topological dynamics of the array under various influences, it was shown that kink-antikink pairs dominate between the HVR and LVR, and the kink instability at high velocities leads to the hysteresis effect [22]. Also, rich spatiotemporal behaviors were revealed in these regimes [18]. It is our task in this paper to study in depth the collective *topological* dynamics of the damped case under the influence of a constant force. In this paper, a *dynamical contraction factor* and *deviation factor* are introduced, which serve as valuable order parameters in describing the motion of the system in a unified way. These two factors in fact originate from the same coherence function, while they possess completely different physical meanings. A dynamical bifurcation from the kink motion to kink-antikink collisions is found in terms of the temporal oscillation of the dynamical contraction factor. This bifurcation closely relates to changes in the spatiotemporal dynamics of the array. The kink loses its stability via a cascade of transitions from the moving kink to the emergence of antikinks.

The arrangement of the present paper is as follows. In Sec. II, a dynamical contraction factor is introduced to describe the dynamics of the topological compression of the

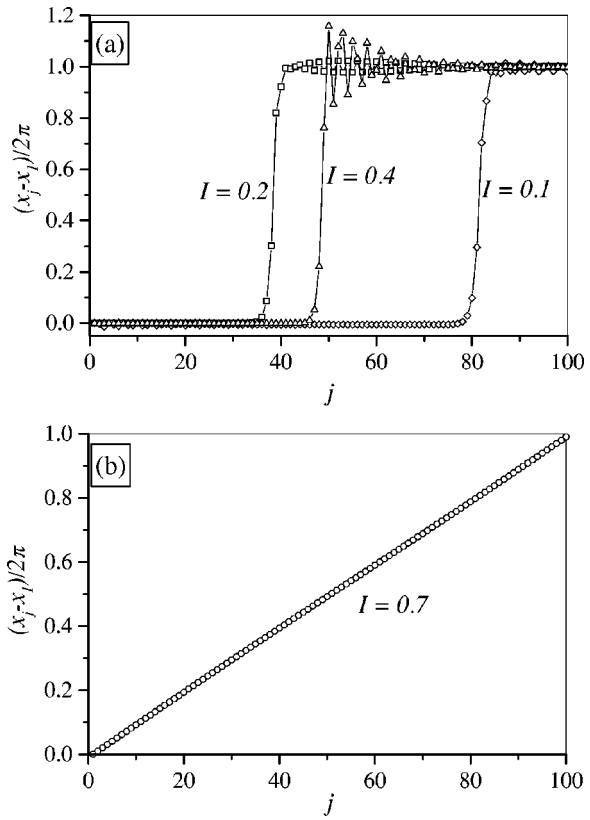

FIG. 1. Two types of kinks. The configuration in (a) is a localized kink, lying in the LVR, and the topological structure in (b) is an extended kink in the HVR. Oscillations in (a) can also be observed on the tail of the kink.

kink, and a deviation factor is also applied to measure the deviation of the velocity-force characteristics from the linear Ohm's law. We investigate the time-averaged behaviors varying with the external driving force. Temporal behaviors of these two quantities are presented in Sec. III, where we connect their temporally collective behaviors with spatiotemporal patterns of the system. We show that the generation of the kink-antikink pairs may reduce the localization of the array, and the collision between kinks and antikinks would lead to strong oscillations of the array. Section IV gives a concluding remark. Throughout the paper $\gamma=0.1$ (the underdamped case) and $K=1.0$ (moderate coupling) are adopted. Periodic boundary conditions are considered, i.e., $\theta_{j+N}(t)=\theta_j(t)+2\pi M$, where M is the number of geometric kinks (twists) trapped in the array. Thus the frustration $\delta=M/N$, and the static length of the harmonic chain should be $\alpha=2\pi\delta$.

II. THE CONTRACTION AND DEVIATION BEHAVIORS

The motion of the FK array under the driving of the dc external force I is dominated by the collective kink motion. In Fig. 1, topological configurations of the array at some time $t=t_0\gg 1$ are given for different driving forces for $N=100$ and $M=1$. For relatively small I, it is shown in Fig. 1(a) that almost all particles are localized at 0 or 1, i.e., a particle may stay in the potential well for a long time before it jumps to another well. As one particle jumps into a new well, the adjacent particles follow this jump due to the harmonic coupling. This type of collective stick-slip motion has been well studied for coupled systems. The oscillatory tails around the 2π kink can be observed in Fig. 1(a). This oscillation is a consequence of the discreteness of the lattice [20]. Under certain conditions, the kink motion and radiated phonon waves may become phase-locked, leading to quantized velocity steps under the driving force I. For very large I, the kink is strongly extended, as shown in Fig. 1(b), where particles are distributed almost uniformly between 0 and 1. The distinct difference between Figs. 1(a) and 1(b) implies a drastic transition in the topology of the array.

To describe the topological behavior of the array, it is instructive to introduce the following coherence function:

$$R(t)\exp[i\varphi(t)]=\frac{1}{N}\sum_{j=1}^{N}\exp[i\theta_j(t)], \tag{3}$$

where $R(t)$ is a typical coherence factor in studies of phase entrainment of coupled limit cycles [7,21]. $\varphi(t)$ denotes a collective phase and i denotes the imaginary index. By separating the real and the imaginary parts $\beta_{1,2}(t)$, one may rewrite the above expression as follows:

$$\beta_1(t)=\frac{1}{N}\sum_{j=1}^{N}\cos[\theta_j(t)], \tag{4}$$

$$\beta_2(t)=\frac{1}{N}\sum_{j=1}^{N}\sin[\theta_j(t)]. \tag{5}$$

The time average of $\beta_{1,2}(t)$ can be accordingly defined:

$$\langle\beta_i(t)\rangle=\lim_{T\to\infty}\frac{1}{T}\int_0^T\beta_i(t)dt,\quad i=1,2. \tag{6}$$

It is interesting that the formula of $\beta_1(t)$ is very similar to the definition of the contraction factor β_{MF} introduced in [17], and $\beta_1(t)$ depicts the dynamical features of the topology of the lattice. Therefore, we call $\beta_1(t)$ the *dynamical contraction factor* (DCF). Usually the value of β_1 lies between 0 and 1. A larger β_1 implies a stronger localization of the kink, as shown in Fig. 1(a). For a very small I, one may expect

$$\langle\beta_1(t)\rangle\approx\beta_{\mathrm{MF}}. \tag{7}$$

In Fig. 2, $\langle\beta_1\rangle$ is plotted by *adiabatically* varying I for cases $\delta=1/100$ and $34/89$ $[\approx(3-\sqrt{5})/2]$. The hysteresis loop can be clearly observed. For $\delta=1/100$ in Fig. 2(a), when I is not large, $\langle\beta_1\rangle$ remains almost constant, whose value is approximately equal to β_{MF}. This is in agreement with the expectation 7 . As one further increases I, a decrease of $\langle\beta_1\rangle$ may be observed, indicating that the array becomes less localized, while a localized kink solution still persists. An abrupt transition occurs at $I\approx 0.65$, where $\langle\beta_1\rangle$ suddenly drops to a small negative value. This change corresponds to the transition from the LVR to the HVR, where the localized kink becomes extended. When I becomes very large, the harmonic array moves uniformly with the velocity $\Omega=I/\gamma$ along the periodic potential. One may approximately write the steady solution of Eq. (1) as $\theta_j(t)=\psi+\alpha j+(I/\gamma)t$,

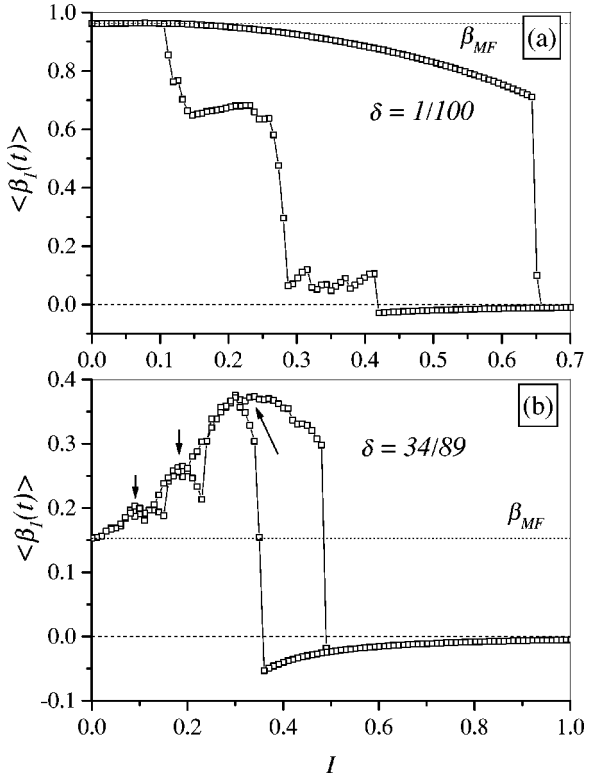

FIG. 2. The relation between the average DCF $\langle\beta_1(t)\rangle$ and the external dc drive I for (a) $\delta=1/100$ and (b) $\delta=34/89$. A decrease in (a) in the LVR can be clearly observed, while in (b) the relation exhibits a multiple-peak behavior (see the regions denoted by arrows) originating from the resonant behavior between the moving kink and the radiated phonon waves. In the multistable region, several different regimes can be identified.

where ψ is an arbitrary constant phase. As $I\to\infty$, by inserting it into Eqs. (4) or (2), we may easily get

$$\beta_1(t)=\mathrm{Re}\left\{\frac{1}{N}\sum_{j=1}^{N}\exp[i\theta_j(t)]\right\}=0. \tag{8}$$

For a finite I, as shown in Fig. 2, $\beta_1<0$, which is not a finite-size effect and depends on $\delta=M/N$. The negative contraction factor corresponds to another type of weak localization different from the low-velocity kink. β_1 approaches 0 when I is increased to infinity. It is shown in Fig. 3 for different frustrations that $\langle\beta_1(t)\rangle$ vs I obeys the same power law:

$$\langle\beta_1(t)\rangle\propto -I^{-2.0}. \tag{9}$$

As one adiabatically decreases I from a large value, $\langle\beta_1\rangle$ jumps to a positive value at $I\approx 0.42$, and several intermediate transitions to higher values occur by further decreasing I. These intermediate states occur beyond the LVR and HVR. Each step denotes a robust topology of the array due to the resonance. When I is decreased to approximately 0.1, $\langle\beta_1\rangle$ jumps back to the low-velocity branch.

Similar transition is also shown for $\delta=34/89$ in Fig. 2(b), with a much larger negative value in the HVR. For the case $\delta=34/89$, there exists a large parameter region of I in the LVR that the $\langle\beta_1\rangle$ is much higher than the ground-state

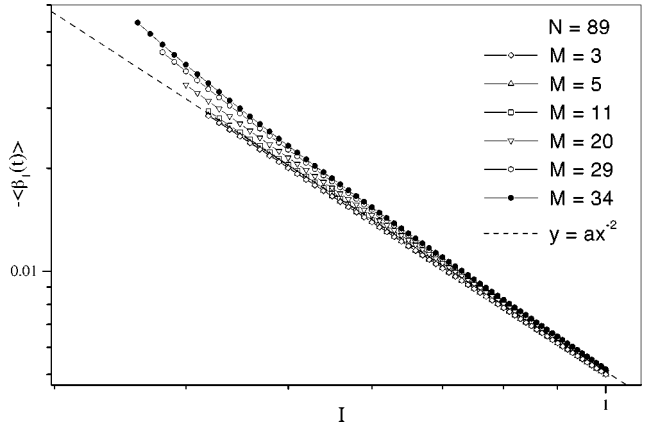

FIG. 3. The same relation as Fig. 3 in the HVR. The axes are labeled by the logarithm scale. Power law can be clearly seen. A fitting line is also drawn for an easy observation.

value β_{MF} [see the part above the dashed line in Fig. 2(b)]. The increase of the contraction factor indicates that the array is further localized as an external driving is applied. This stronger localization comes from the interaction of the multiple trapped kinks (i.e., $M>1$) and the phonons, and a reasonable theoretical interpretation of this collective suppression is still open. The DCF becomes the largest in the interval $I\approx 0.3-0.35$ and decreases as one goes on adiabatically increasing I.

Now let us focus on the discussion of $\beta_2(t)$. Under a given external force I, $\dot{\theta}_j(t)$ oscillates around the averaged phase velocity Ω. One expects the time average of $\ddot{\theta}_j(t)$ may have small contributions, i.e., $\langle\ddot{\theta}_j(t)\rangle\approx 0$. By averaging Eq. (1) over both time and lattices on both hands and omitting the second-derivative term, we get $\gamma\Omega+(1/N)\Sigma_j\langle\sin\theta_j(t)\rangle=I$. Recalling the definition of $\beta_2(t)$, one obtains

$$\langle\beta_2(t)\rangle=\frac{1}{N}\sum_j\langle\sin\theta_j(t)\rangle=I-\gamma\Omega. \tag{10}$$

For a large driving I, the motion of the array obeys an Ohm's law, i.e., $\Omega=I/\gamma$ and $\langle\beta_2(t)\rangle=0$. Therefore, $\langle\beta_2(t)\rangle$ in fact describes the deviation of the system from this linear velocity-force relation. We call this quantity the *deviation factor* (DF). In Fig. 4 we give relations $\langle\beta_2\rangle-I$ for $\delta=1/100$ and 34/89. A large parameter region shows a deviation from the Ohm's law (see the nonzero DF in Fig. 4). This deviation behavior comes from the resonance between the moving kink and its radiated phonon waves, leading to a weak dependence of Ω on I. It is interesting to note that in the HVR, we have $\langle\beta_2\rangle=0$ while $\langle\beta_1\rangle\neq 0$. This indicates that although the motion of the array obeys the linear velocity-force law, the *topology* of the array still ''feels'' the periodic substrate due to the discreteness of the lattice. In Fig. 4, theoretical lines are shown by dashed lines. The agreement between the numerical simulation and theoretical argument is quite good.

It is interesting that the hysteresis effect manifests itself in the topological structure of the array. This indicates that hysteresis in the velocity (or, mobility) force characteristics results from the structural robustness of the array. Especially,

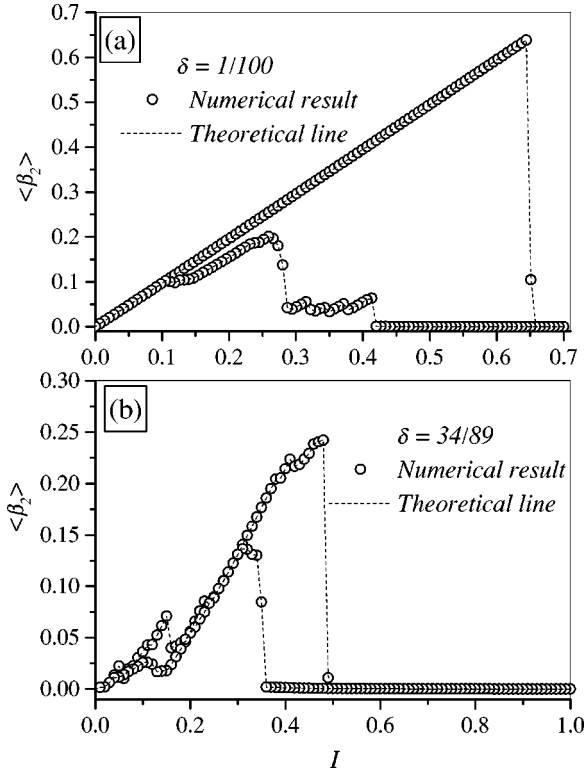

FIG. 4. The average DF $\langle\beta_2(t)\rangle$ varies with the external dc force I, where $\delta=1/100$ in (a) and $\delta=34/89$ in (b). Linear deviations from the linear Ohm's law are clearly shown. The dashed theoretical lines $\langle\beta_2\rangle=I-\gamma\Omega$ are in perfect agreement with numerical results.

the topology of the array still persists as weak noises are applied. This has been numerously tested in simulations.

III. KINK-ANTIKINK INTERACTION INDUCED DYNAMICAL TRANSITIONS

To explore the dynamics of the system and get a better understanding of topological changes described above, it is pertinent to investigate the temporal behaviors of these two factors. In Fig. 5, we give the time evolution of $\beta_{1,2}(t)$ for $I=0.1$, 0.2, 0.4, and 0.5. Initial values are randomly given. For small I, both $\beta_1(t)$ and $\beta_2(t)$ approach positive values with very small-amplitude oscillations. As I increases, the temporal behavior of these factors becomes complicated. When I changes from 0.1 to 0.2, large-amplitude pulselike oscillations are superimposed on the small oscillation background, and meanwhile the average values $\langle\beta_{1,2}(t)\rangle$ decrease. With further increasing I, the large-amplitude oscillation occurs more frequently. This type of oscillation implies strong fluctuations in the topology of the kink, signifying a dynamical bifurcation to a new topological state. To reveal the origin of this oscillation, let us explore the spatiotemporal behavior of the system. In Figs. 6(a)–6(d), we plot the spatiotemporal patterns corresponding to cases in Figs. 5(a)–5(d) with the same initial conditions. The black line represents lower values of $\cos[\theta_j(t)]$. A moving kink can be clearly observed. In Fig. 6(b) for $I=0.2$, antikinks, which propogate toward the opposite direction of kinks, can be found. In Fig. 7, a profile of the configuration of the array is

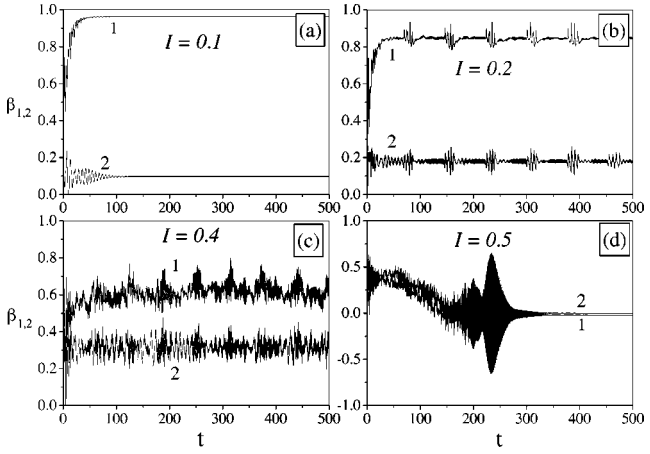

FIG. 5. Time evolution of the DCF $\beta_1(t)$ for $N=100$ and $M=1$ for different cases: (a) $I=0.1$; (b) $I=0.2$; (c) $I=0.4$; (d) $I=0.5$. From (b) to (d), one may notice the large-amplitude fluctuation around an average value, resulting from the kink-antikink interactions. More frequent flutuations indicate higher concentration of the kink-antikink pairs. In (d), the contraction factor decreases to a small negative value, indicating the transition to the HVR.

given at some time $t=t_0$ for $I=0.2$, $N=100$, and $M=1$. As compared to Fig. 1(a), the configuration possesses a hump and a valley, which are composed of three kinks and two antikinks. This observation coincides with the spatiotemporal pattern in Fig. 6(b), where there are three lines with the negative slope and two lines with positive slope. An antikink describes the minimally possible, topologically stable *extension* of the commensurate structure [22,23]. The localized kink is stretched due to the presence of antikinks, thus $\langle\beta_1(t)\rangle$ decreases. This interprets the behavior of the average DCF in Fig. 5. The antikink moves toward the *opposite* direction of the kink motion and collides with kinks. As soon as a kink collides with an antikink, the $\beta_{1,2}(t)$ experience strong oscillations in a pulsed manner. More kink-antikink pairs are generated and collisions occur more frequently when the driving force I increases. This leads to stronger

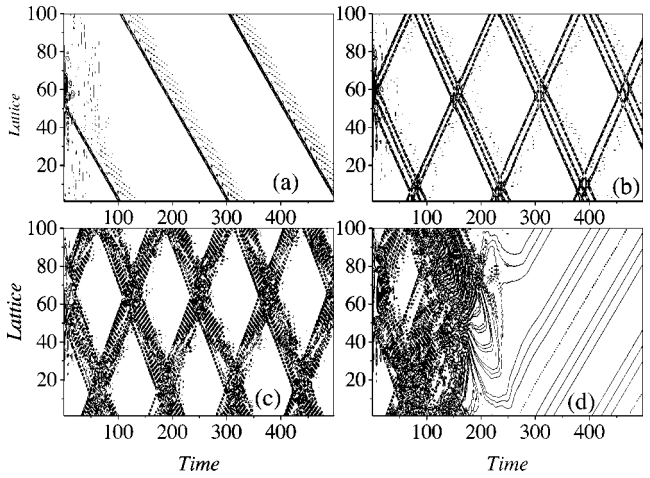

FIG. 6. The spatiotemporal patterns corresponding to the cases in Fig. 2. Collisions of kinks and antikinks can be observed from (b), and the interactions become more frequent with increasing the dc force I in (c). In (d), kink-antikink collisions induce an avalanche, finishing in a totally running state.

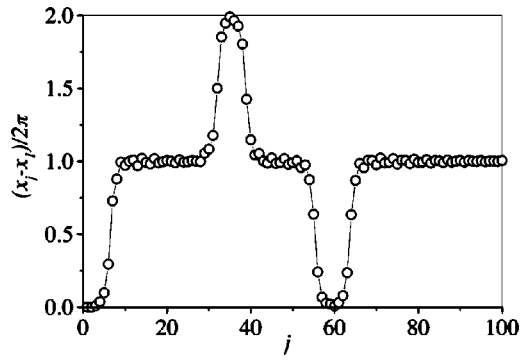

FIG. 7. A profile of the configuration of the array for $N=100$, $M=1$, and $I=0.2$. Different from the topology for $I=0.2$ in Fig. 1(a), antikinks are observed.

pulselike oscillations. At the same time the average contraction factor decreases due to the stretching effect of antikinks. In Fig. 6(d), we give a case at the onset of the transition from the LVR to HVR. One may find that many kink-antikink pairs are generated, and meanwhile collisions between kinks and antikinks excite more pairs. This avalanche behavior eventually leads to a complete extension of the array [22]. The avalanche in Fig. 6(d) corresponds to the decrease of $\beta_1(t)$ [$\beta_2(t)$] to a small negative value (zero) in Fig. 5(d). A very strong oscillation in the interval $t=200-300$ indicates a drastically frequent collision of kinks and antikinks. In Fig. 8 we show the loss of stability of the kink by plotting the evolution of the DCF and the spatiotemporal pattern for $F=0.7$, $N=100$, and $M=1$. The system evolves from the ground state ($F=0$, $\dot{\theta}_j=0$). When a large force is applied at $t=0$, the trapped kink begins to move along the chain. This leads to a drastic oscillation of $\beta_1(t)$, whose minimum values decrease through zero and touch the negative zone. The phase velocity of the array increases with the time. For high velocities, the kink

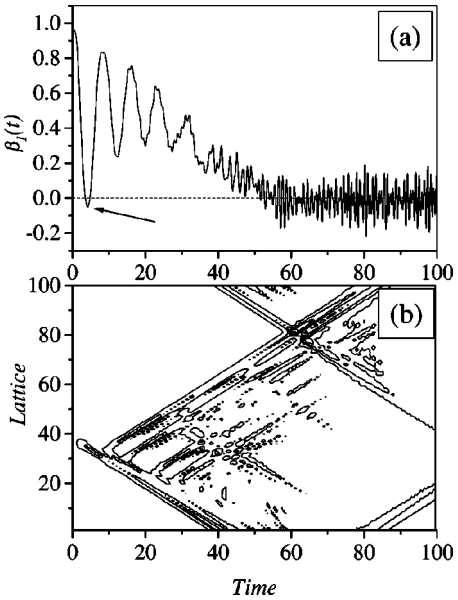

FIG. 8. (a) The evolution of $\beta_1(t)$ for $I=0.7$ and $N=100$, $M=1$. (b) The corresponding spatiotemporal pattern. Antikinks bifurcate from the moving kink, corresponding to the peaks of $\beta_1(t)$.

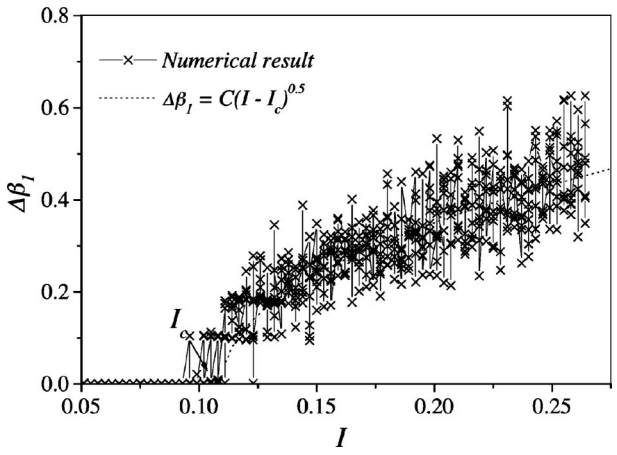

FIG. 9. The oscillation amplitude of the DCF against the external dc force. A bifurcation from the localized kink state to the kink-antikink-pair state is observed with the scaling exponent $\xi=0.5$.

solution loses its stability by bifurcating the first antikink. The second dynamical bifurcation takes place at $t\approx15$, where another antikink is excited. At $t\approx22$ and 28, the third and fourth antikinks bifurcate from the dominating kink. A cascade of kink-antikink emergence leads to the extension of the array. The excited bundles of kinks and antikinks collide and excite more pairs. As the dominant kink and antikink bundles collide at $t\approx60$, the chain becomes fully extended, corresponding to a drastic decrease of $\beta_1(t)$ to zero. This dynamical bifurcation cascade implies a cascade of losses of stability of kink and kink-antikink states, which manifests on the evolution of $\beta_1(t)$ (note the first four peaks corresponding to the bifurcation points). A theoretical study of this scenario of bifurcations is very important in understanding the hystersis behavior. This is under exhaustive investigations now.

To better show the dynamical transition from the kink state to the kink-antikink-pair state, it is intuitive to quantitatively investigate the oscillation behavior of $\beta_1(t)$. We rewrite $\beta_1(t)=\langle\beta_1\rangle+\Delta\beta_1(t)$ and $\Delta\beta_1=\max|\Delta\beta_1(t)|$. In Fig. 9, we give the relation between $\Delta\beta_1$ and I for the case $\delta=1/100$. It can be found that at $I=I_c$, a new positive branch bifurcates from the nearly zero branch with the scaling law,

$$\Delta\beta_1\propto(I-I_c)^{\xi}, \tag{11}$$

where the exponent $\xi\simeq0.5$. As shown in Fig. 6, the large pulselike oscillations originate from the interaction of kinks and antikinks. Therefore, this dynamical bifurcation just corresponds to the emergence of kink-antikink pairs. The nonzero branch may coexist with the kink-antikink branch in a large parameter regime of I due to the multistability of the system. The kink-antikink states correspond to intermediate states between the localized kink (LVR) and extended kink (HVR) states. On this branch, more kink-antikink pairs can be excited as one increases I, and this in consequence leads to the strong fluctuation of the topological configuration of the array and the relaxation of the kink compression.

IV. CONCLUDING REMARKS

It is an interesting and important issue to introduce an appropriate quantity to characterize the topology of the array. In this paper, we define a dynamical contraction factor to describe the topological change of the kink and a deviation factor to depict the nonlinear effect of the velocity-force relation. These two quantities are closely connected with the coherence factor, while they have purely different physical implications. We show that the average DCF exhibits transitions corresponding to topological changes. The kink is further compressed when it moves for the incommensurate case. In the HVR, we show that although the motion of the array on average obeys the Ohm's law, the topology still feel the substrate. A cascade of dynamical bifurcation from the kink to kink-antikink and extended states is shown. We also give the scaling law of the kink-antikink transition. We also studied their temporal features by resorting to the spatiotemporal pattern dynamics of the system, and found that the kink-antikink interaction may result in strong oscillations of these two functions.

The parameters we introduced in this paper are very useful in explorations of collective dynamics of coupled oscillators. On the other hand, because these two quantities relate to the average on lattices, the detailed dynamics of local lattices cannot be accurately studied by applying them one at a time. A collaboration of spatiotemporal patterns and the DCF (DF) is necessary.

Because the Frenkel-Kontorova model corresponds to a number of real situations such as charge-density waves, Josephson junction arrays and ladders, coupled pendula, and so on, the method and behaviors proposed in this paper are expected to be well applied to these experimental studies.

ACKNOWLEDGMENTS

This work is supported in part by the Research Grant Council (RGC) and the Hong Kong Baptist University Faculty Research Grant (FRG). Z.Z. acknowledges support from the National Natural Science Foundation of China, the Special Funds for Major State Basic Research projects and the Foundation for Excellent Teachers from the Educational Bureau of China.

[1] H. Haken, *Advanced Synergetics* (Springer, Berlin, 1983).
[2] M. C. Cross and P. C. Honenberg, Rev. Mod. Phys. **65**, 851 (1993).
[3] B. N. J. Persson, Phys. Rev. Lett. **71**, 1212 (1993); J. Chem. Phys. **103**, 3849 (1995).
[4] S. H. Strogatz, *Nonlinear Dynamics and Chaos* (Addison-Wesley, Reading, MA, 1994).
[5] L. Floria and J. Mazo, Adv. Phys. **45**, 505 (1996).
[6] A. T. Winfree, *The Geometry of Biological Time* (Springer, Berlin, 1980).
[7] Y. Kuramoto, *Chemical Oscillations, Waves, and Turbulence* (Springer, Berlin, 1984).
[8] J. Frenkel and T. Kontorova, Phys. Z. Sowjetunion **13**, 1 (1938).
[9] M. Remoissenet, *Waves Called Solitons, Concepts and Experiments* (Springer-Verlag, Berlin, 1994).
[10] D. S. Fisher, Phys. Rev. Lett. **50**, 1486 (1983); Phys. Rev. B **31**, 1396 (1985); L. Sneddon and K. Cox, Phys. Rev. Lett. **58**, 1903 (1987); L. Sneddon and S. Liu, Phys. Rev. B **43**, 5798 (1991); S. Coppersmith, *ibid.* **30**, 410 (1984); S. Coppersmith and D. Fisher, Phys. Rev. A **38**, 6338 (1988).
[11] *Physics of Sliding Friction*, edited by B. N. J. Persson and E. Tosatti (Kluwer Academic Publishers, Dordrecht, 1996); Y. Braiman, F. Family, and H. G. E. Hentschel, Phys. Rev. E **53**, R3005 (1996).
[12] B. Hu, B. Li, and H. Zhao, Phys. Rev. E **57**, 2992 (1998).
[13] Y. Braiman, W. L. Ditto, K. Wiesenfeld, and M. L. Spano, Phys. Lett. A **206**, 54 (1995); Y. Braiman, J. Lindner, and W. L. Ditto, Nature (London) **378**, 465 (1995).
[14] Z. Csahok, F. Family, and T. Vicsek, Phys. Rev. E **55**, 5179 (1997); A. V. Savin *et al.*, Phys. Lett. A **229**, 279 (1997).
[15] S. Watanabe, H. Zant, S. Strogatz, and T. Orlando, Physica D **97**, 429 (1996); A. Ustinov, M. Cirillo, and B. Malomed, Phys. Rev. B **47**, 8357 (1993); **51**, 3081 (1995); L. Floria and F. Falo, Phys. Rev. Lett. **68**, 2713 (1992).
[16] W. Selke, Phys. Rep. **170**, 213 (1988); S. Aubry, *ibid.* **103**, 12 (1984); M. Peyrard and S. Aubry, J. Phys. C **16**, 1593 (1983).
[17] Z. Zheng, B. Hu, and G. Hu, Phys. Rev. E **57**, 1139 (1998); Phys. Rev. B **58**, 5453 (1998).
[18] T. Strunz and F. J. Elmer, Phys. Rev. E **58**, 1601 (1998); **58**, 1612 (1998).
[19] Z. Zheng, B. Hu, and G. Hu, Phys. Rev. E **58**, 7085 (1998).
[20] M. Peyrard and M. Kruskal, Physica D **14**, 88 (1984); J. Currie, S. Trullinger, A. Bishop, and J. Krumhansi, Phys. Rev. B **15**, 5567 (1977); R. Boesch, C. R. Willis, and M. El-Batanouny, *ibid.* **40**, 2284 (1989).
[21] H. Daido, Phys. Rev. Lett. **61**, 231 (1988); Z. Zheng, G. Hu, and B. Hu, *ibid.* **81**, 5318 (1998).
[22] O. M. Braun, A. R. Bishop, and J. Roder, Phys. Rev. Lett. **79**, 3692 (1997).
[23] X. Weiner, O. Braun, T. Dauxois, M. Paliy, and M. Peyrard, Phys. Rev. Lett. **78**, 1295 (1997); Phys. Rev. E **55**, 3598 (1997); O. Braun and Y. Kivshar, Phys. Rev. B **44**, 7694 (1991); **50**, 13 388 (1994).